Zinc oxide nanoparticles potentiate the antibacterial and antibiofilm efficacy of imipenem against *Klebsiella pneumoniae*

Deyar Jassim Shawi[A,B], Ayaid Khadem Zgair[A,C–F]

Department of Biology, College of Science, University of Baghdad, Iraq

A – research concept and design; B – collection and/or assembly of data; C – data analysis and interpretation;
D – writing the article; E – critical revision of the article; F – final approval of the article

Polymers in Medicine, ISSN 0370-0747, eISSN 2451-2699 *Polim Med*. 2026;56(1):53–63

Address for correspondence
Ayaid Khadem Zgair
E-mail: ayaid.zgair@sc.uobaghdad.edu.iq

Funding sources
None declared

Conflict of interest
None declared

Acknowledgements
The authors thank all staff members of the Department of Biology, College of Science, University of Baghdad, for their support during the experimental work. Furthermore, the authors thank the hospitals and clinical laboratories that helped the researchers isolate and identify the bacterial isolates.

Received: February 7, 2026
Revised: March 4, 2026
Accepted: March 30, 2026
Final review: March 6, 2026

Published online on June 30, 2026

Abstract

Background. Biofilm extracellular polymeric matrix (EPS) biomass plays a central role in bacterial resistance to carbapenems, especially imipenem (IPM), which poses a serious threat to public health.

Objectives. The present study aims to use ZnO NPs to improve the susceptibility of imipenem-resistant *Klebsiella pneumoniae* (IRKP) to imipenem (IPM) and to reduce biofilm extracellular polymeric matrix (EPS) biomass.

Materials and methods. Susceptibility to IPM and biofilm formation were evaluated in 20 uropathogenic *K. pneumoniae* isolates. ZnO NPs were prepared using an extract of *Thymus vulgaris* leaves. The effects of sub-minimum inhibitory concentrations (MICs) of IPM and ZnO NPs on biofilm formation were evaluated. The additive effect of sub-MICs of ZnO NPs on IRKP susceptibility to IPM and biofilm formation was assessed.

Results. The diameter of the prepared ZnO NPs was less than 50 nm. Biofilm formation negatively correlated with inhibition zone diameter ($r = -0.819$, $p = 0.001$) and positively with IPM MICs ($r = 0.79$, $p = 0.001$). Sub-MICs of IPM and ZnO NPs reduced biofilm formation on polystyrene in a concentration-dependent manner. The synergistic role of sub-MICs of ZnO NPs in decreasing the MICs of IPM against *K. pneumoniae* was observed, from 250 ± 50 µg/mL to 116.6 ± 14.4 µg/mL (at ½, ¼, and ⅛ MICs of ZnO NPs), while 1⁄16 MIC of ZnO NPs decreased the MICs of IPM to 125 ± 25 µg/mL. The 1⁄32 and 1⁄64 MICs of ZnO NPs reduced the MICs of IPM to 141.6 ± 14.4 µg/mL and 158.3 ± 80.36 µg/mL, respectively. The greatest reduction in biofilm extracellular polymeric matrix (EPS) formation was observed at the highest concentrations of the IPM/ZnO NP combination, while the lowest reduction was observed at the lowest concentrations of both materials ($p < 0.05$).

Conclusions. The present study demonstrated a synergistic effect of sub-MIC ZnO NPs on the antibacterial and antibiofilm activities of imipenem against *K. pneumoniae* (IRKP).

Key words: *Klebsiella pneumoniae*, ZnO NPs, imipenem, biofilm formation

Cite as
Shawi DJ, Zgair AK. Zinc oxide nanoparticles potentiate the antibacterial and antibiofilm efficacy of imipenem against *Klebsiella pneumoniae*. *Polim Med*. 2026;56(1):53–63. doi:10.17219/pim/220166

DOI
10.17219/pim/220166

Background

Biofilm-associated infections with this bacterial species are difficult to treat because the extracellular polymeric matrix (EPS) of the biofilm acts as a barrier, reducing antibiotic penetration and promoting bacterial resistance.[1] Therefore, new strategies to reduce biofilm formation may help limit and enhance the activity of antibiotics against resistant bacteria. New approaches in materials science have focused on polymers and nanoparticles (NPs) as multifunctional platforms for antibacterial applications.[2] Natural and synthetic polymers play a significant role in the design of functional nanoparticles, which serve as stabilizers, carriers, or surface modifiers. Polymeric materials can modify nanoparticle size, surface charge, dispersibility, and interactions with biological cellular processes; they can improve biocompatibility and antimicrobial activity.[3] Furthermore, polymer–nanoparticle composites offer tunable physicochemical properties that can be used to disrupt bacterial membrane systems, alter biofilm structure, and improve drug activity in terms of delivery efficiency against bacterial cellular processes.[4]

The rise in antimicrobial resistance among Gram-negative pathogens has become a critical global health concern, especially during periods of limited availability of effective antibiotics. Imipenem (IPM) is a beta-lactam antibiotic commonly used to treat infections caused by multidrug-resistant (MDR) organisms, including *Klebsiella pneumoniae*.[5] This bacterial species is an opportunistic pathogen responsible for several infectious diseases, including wound and soft tissue infections, pneumonia, bloodstream infections (septicemia), liver abscess (invasive *Klebsiella* syndrome), eye infections, and urinary tract infections (UTIs).[6] The resistance of this bacterial species to a wide spectrum of antibiotics and its ability to adhere to biotic and abiotic surfaces (forming biofilms) are associated with increased virulence.[7]

Metal oxide nanoparticles are of great importance due to their antimicrobial properties and multiple effects on cellular processes. One of the most important is zinc oxide (ZnO) nanoparticles, valued for their chemical stability, low cost, and recognized biocompatibility in biological systems. ZnO NPs exhibit broad-spectrum antibacterial activity via multiple mechanisms, including the production of reactive oxygen species, disruption of bacterial cell membranes, and the release of Zn^{2+} ions, which interfere with bacterial metabolic processes.[8] On the other hand, the nanoscale size of ZnO NPs and their high surface-to-volume ratio facilitate interactions with bacterial metabolism and the polymers of biofilm matrices.[9]

The combination of nanoparticles with polymer-based systems disrupts bacterial cell function by controlling nanoparticle aggregation and enhancing interactions with microbial populations, including the biofilm matrix. This process has shown that nanoparticles can more effectively penetrate biofilm matrices and improve antibiotic activity.[10] Thus, combining nanoparticles with antibiotics can act synergistically by increasing bacterial cell membrane permeability, reducing efflux pump activity, and facilitating antibiotic penetration into the biofilm matrix.[11]

Objectives

The additive antibacterial and antibiofilm effects of ZnO NPs on imipenem activity are highlighted, underscoring the roles of material properties and nanoscale interactions in improving antibacterial outcomes. This approach demonstrates a new strategy to enhance imipenem activity against imipenem-resistant *K. pneumoniae*, a serious public health threat.

Materials and methods

Ethical approval

The study was approved by the Human Ethics Committee of the Department of Biology, College of Science, University of Baghdad, Iraq, with reference No. CSEC/1025/0112, on October 9, 2025.

Bacterial isolates

Aseptic midstream urine samples were collected from 183 patients diagnosed with urinary tract infections (UTIs) who attended Al-Yarmouk Teaching Hospital, Baghdad, Iraq, for routine clinical evaluation. Patients who had received antibiotic therapy within 72 h prior to sample collection were excluded, and informed consent was obtained from all participants. The urine samples were cultured on MacConkey agar (HiMedia, Mumbai, India) and incubated at 37°C for 18 h. Large, mucoid, pink colonies (lactose-fermenting colonies) were selected for further identification. Gram staining was performed, followed by biochemical tests, including oxidase, indole, urease, and citrate utilization tests. A VITEK DensiCheck instrument and fluorescence system (bioMérieux, Marcy-l'Étoile, France) (ID-GNB card) were used to identify the isolates as *K. pneumoniae*. All confirmed *K. pneumoniae* isolates were stored at –80°C in tryptic soy broth (TSB) supplemented with 20% (v/v) glycerol for long-term preservation until further use.

Kirby–Bauer method

This method was used to determine the response of *K. pneumoniae* isolates to imipenem (IPM). Bacterial suspensions were prepared and adjusted to a turbidity equivalent to a 0.5 McFarland standard and then uniformly inoculated onto Mueller–Hinton agar (MHA; HiMedia, India). Imipenem disks were placed on the MHA surface, and

the plates were incubated for 18 h at 37°C. Inhibition zones were measured in millimeters. Inhibition zone diameters were measured as the total diameter, including the 6 mm disk diameter, in accordance with Clinical and Laboratory Standards Institute (CLSI) guidelines. The isolates were categorized as susceptible (S), intermediate (I), or resistant (R) to IPM based on CLSI breakpoints.[12,13]

ZnO NPs preparation

The previously described standard method was followed for biosynthesis using Thymus vulgaris leaves purchased from local markets in Baghdad, Iraq. The leaves were washed several times to remove dust, then dried and ground into a powder. Fifty grams of the powder were added to 500 mL of distilled water and heated to 80°C for 45 min. The mixture was cooled to room temperature and filtered through Whatman filter paper (No. 1) to remove solids. The clear suspension was stored at 4°C until use.[14]

Fifty milliliters of the leaf extract were added dropwise to a 0.1 M $Zn(NO_3)_2{\cdot}6H_2O$ (Sigma-Aldrich, St. Louis, USA) solution prepared in deionized double-distilled water (1:1, v/v). The reaction was carried out at ambient room temperature (21°C), maintained in the laboratory without the use of an incubator, under continuous magnetic stirring (Heidolph Instruments, Germany). The pH was adjusted to 8 with 0.1 M NaOH until the mixture turned milky white and was then heated at 80°C for 3 h to obtain a brownish paste. The sedimented growth fluid was separated from the ZnO NPs by centrifugation at 7,000 × g for 10 min (Benchtop High Speed Centrifuge CFG-17H, Scitek, China). The solid powder was removed using methanol. Following the ethanol wash, distilled water was used several times to further wash the ZnO NPs. The ZnO NPs were dried in an oven (Memmert GmbH, Schwabach, Germany) at 70°C until completely dry.[14]

The prepared ZnO NPs were characterized using atomic force microscopy (AFM; Innova® AFM; Bruker, Santa Barbara, USA). For AFM analysis, a thin film of the nanoparticles was deposited on a glass substrate. Scanning electron microscopy (SEM) was also performed (Zeiss EVO® LS 15; Carl Zeiss AG, Jena, Germany); a smear of ZnO NPs was prepared on a glass surface and coated with a thin layer of platinum to enhance conductivity for imaging.[14,15]

MTT assay

In this method, the cytotoxicity of ZnO NPs on MCF-7 human breast cancer cells was evaluated using the MTT assay, a colorimetric indicator of cell viability. MCF-7 cells (ATCC) were cultured in RPMI-1640 medium (Sigma-Aldrich, USA) supplemented with 10% fetal bovine serum (FBS, Sigma-Aldrich, USA) and 1% penicillin/streptomycin (MSE SAS, France) and maintained at 37°C in a humidified atmosphere containing 5% CO_2. Cells were seeded into 96-well tissue culture plates at a density of 10^4 cells/well, incubated overnight, and then treated under the above conditions for 24 h and 72 h.[16]

A stock solution of ZnO NPs was prepared, and serial two-fold dilutions were made in complete culture medium (100, 50, 25, 10, 5, and 1 µg/mL). The negative control consisted of untreated cells cultured in medium alone. The growth medium was removed, and 100 µL of medium containing ZnO NPs was added, followed by incubation for 24 h under standard culture conditions. Following treatment, the medium was discarded, and 20 µL of MTT solution (1 mg/mL) was added to each well and incubated for 4 h at 37°C to allow viable cells to reduce MTT into insoluble purple formazan crystals. (Note: the 4 h incubation refers specifically to the formazan development step, not the treatment duration). The MTT solution was then removed, and 100 µL of dimethyl sulfoxide (DMSO) was added to dissolve the formazan crystals. Absorbance was measured at 570 nm using a microplate reader (Bio-Rad, USA).[17,18] Cell viability was expressed as a percentage relative to untreated control cells using the following formula:

$$\text{Cell viability}\left(\%\right) = \left(\frac{\text{Abs}_{\text{treated}}}{\text{Abs}_{\text{control}}}\right) \times 100$$

Minimum inhibitory concentrations

The broth microdilution method was used to determine the minimum inhibitory concentrations (MICs) of IPM and ZnO NPs against *K. pneumoniae* isolates. Two-fold serial dilutions of IPM (Medscape, New York City, USA) were prepared in Mueller–Hinton broth (MHB; HiMedia, India) in a U-shaped microtiter plate. The standardized bacterial inoculum was adjusted to an optical density of 0.1 at 600 nm, equivalent to approximately 1–2 × 10^8 CFU/mL (0.5 McFarland standard), and then diluted 1 : 100 in MHB to achieve a final inoculum of approximately 5 × 10^5 CFU/mL per well, consistent with CLSI M07 broth microdilution guidelines. Five microliters of *K. pneumoniae* suspension were added to each well. The bacterial suspension was prepared by washing the overnight growth of *K. pneumoniae* with sterile phosphate-buffered saline (PBS; 0.1 M, pH 7.2) using centrifugation at 6,500 × g for 10 min (Benchtop High Speed Centrifuge CFG-17H, Scitek, China). The bacterial suspension was adjusted to an optical density of 0.1 at 600 nm (Thermo Fisher Scientific, USA). Plates were incubated at 37°C for 18 h, and MICs were defined as the lowest concentrations that completely inhibited visible bacterial growth. Three controls were prepared: MHB with bacterial isolate (first control), wells containing MHB only (second control), and two-fold serial dilutions of antibiotic only (third control). A similar method was followed to measure the MICs of ZnO NPs against *K. pneumoniae* isolates.[15,19]

Biofilm formation

In this method, 100 µL of sterile Tryptic Soy Broth (TSB; HiMedia, India) supplemented with 0.25% (w/v) glucose was added to the wells of flat-bottom polystyrene tissue culture plates. TSB was supplemented with 0.25% (w/v) glucose to enhance biofilm formation on polystyrene surfaces, as glucose promotes the production of extracellular polymeric substances. Five microliters of a standard inoculum of *K. pneumoniae* were added to each well (as described in the method for MIC evaluation), and the plates were incubated at 37°C for 24 h. The TSB was discarded, and the plates were washed three times with distilled water. The plates were then dried and stained with 100 µL of 0.4% Hucker crystal violet for 15 min, followed by washing five times with distilled water. After the wells were dried, 100 µL of anhydrous ethanol (Sigma-Aldrich, USA) was added to each well. Absorbance was measured at 590 nm using a microplate reader (BioTek 800 TS; BioTek, Winooski, USA). The experiment was performed in triplicate.[19,20]

Effect of sub-MICs on biofilm formation

In this experiment, the effects of sub-MIC concentrations of IPM and ZnO NPs on biofilm formation by *K. pneumoniae* isolates were investigated. A biofilm formation assay similar to that previously described,[19] with minor modifications, was used. Serial dilutions of sub-MICs of either ZnO NPs or IPM were prepared in TSB (HiMedia, India) and dispensed into the flat-bottom wells of a 96-well polystyrene microtiter plate. Five microliters of a standard *K. pneumoniae* inoculum (as described in the MIC evaluation method) were added to the wells, and the plates were incubated at 37°C for 24 h. Following incubation, the wells were washed three times with distilled water, dried, and stained with 0.4% Hucker crystal violet for 15 min. After drying, anhydrous ethanol was added to each well. Absorbance was measured at 590 nm using a microplate reader (BioTek 800 TS; BioTek, Winooski, USA). The experiment was repeated three times.[19]

Synergistic effect of ZnO NPs and IPM on MICs

The checkerboard microdilution method, performed in a 96-well U-bottom polystyrene microtiter plate, was used to evaluate the synergistic effect of ZnO NPs on the susceptibility (as measured by MICs) of *K. pneumoniae* (resistant to IPM) to IPM. Briefly, 100 µL of sterile MHB (HiMedia, India) was added to each well. Two-fold serial dilutions of IPM were prepared horizontally across the plate (columns 1–12), yielding final concentrations ranging from 1000 to 0.48 µg/mL. Two-fold serial dilutions of ZnO NPs corresponding to sub-MICs (½ MIC to $\frac{1}{128}$ MIC) were prepared vertically from row A to row G. Five microliters of a standard inoculum of *K. pneumoniae* (as described in the MIC preparation method) were added to the wells. The plates were gently shaken and incubated at 37°C for 24 h. The MIC was defined as the lowest concentration of IPM that inhibited visible bacterial growth. Row H was considered the first control, showing the MIC of IPM (without ZnO NPs). Control groups were as follows: first control – IPM serial dilutions without ZnO NPs; second control – bacterial growth control (MHB + bacteria only); third control – sterility control (MHB only); fourth control – ZnO NPs at sub-MIC concentrations with bacterial inoculum without IPM; fifth control – IPM serial dilutions without nanoparticles. The experiment was repeated three times.

Synergistic effect of ZnO NPs and IPM on biofilm formation

A similar procedure was followed to assess the synergistic effect of ZnO NPs on the MICs of IPM against an IPM-resistant *K. pneumoniae* isolate that produced the highest level of biofilm biomass, with minor modifications. TSB was used instead of MHB, and a 96-well flat-bottom polystyrene microtiter plate was used instead of a 96-well U-bottom plate. After incubation, the plates were washed three times with distilled water, dried, and stained with 100 µL of 0.4% Hucker crystal violet for 15 min. After washing and drying, 100 µL of anhydrous ethanol (Sigma-Aldrich, USA) was added to each well. Absorbance was measured at 590 nm using a microplate reader (BioTek 800 TS; BioTek, Winooski, USA). The experiment was repeated three times.[19–21]

Statistical analyses

The statistical analyses and graphs were generated using Origin v. 8.4 (OriginLab, Northampton, USA). The chi-square test was performed using SPSS v. 26 (IBM, USA) for comparisons of categorical resistance data. Data were presented as means ± standard error (M ± SE). Student's t-test and one-way analysis of variance (ANOVA) were used to assess statistical significance. Correlations were evaluated using Pearson's correlation coefficient. A p-value of less than 0.05 was considered statistically significant.

Results

Bacterial isolates and IPM susceptibility

In the present study, twenty *K. pneumoniae* isolates were obtained from 183 urine samples collected from patients with UTIs. The isolates were initially identified using biochemical tests, and species-level identification was subsequently confirmed using the VITEK® 2 system. In the current study, the incidence of UTIs caused by *K. pneumoniae* was 10.92%.

The Kirby–Bauer disk diffusion method showed that the inhibition zone diameters of the twenty *K. pneumoniae* isolates ranged from 7.5 ± 0.8 mm (Kp14) to 31.7 ± 3.2 mm (Kp8). All inhibition zone diameters reported represent the total diameter, including the 6 mm disk diameter, consistent with CLSI measurement guidelines. MIC values were also used to assess the susceptibility of these isolates to IPM. The MICs of IPM against the 20 isolates ranged from 0.24 µg/mL (Kp1, Kp6, Kp8) to 250 µg/mL (Kp4, Kp9, Kp14, Kp20), confirming the inverse relationship between MIC and inhibition zone diameter. The current study indicates variable susceptibility to IPM. Of the 20 isolates, 7 (35%) were susceptible to IPM, 1 (5%) was intermediate (I), and 12 (60%) were resistant to IPM. This finding indicates a high prevalence of IPM resistance. Overall, an inverse relationship between inhibition zone diameter and MIC was observed, supporting the validity of the susceptibility testing (Table 1).

Table 1. Imipenem susceptibility of twenty *K. pneumoniae* isolates, as determined according to CLSI guidelines, and their ability to form biofilms. This table presents inhibition zone diameters (mm), minimum inhibitory concentrations (MIC, µg/mL), and biofilm formation measured as absorbance at 590 nm for the isolates. The isolates were categorized as susceptible (S), intermediate (I), or resistant (R) to IPM based on CLSI breakpoints

No. of isolates	Inhibition zone (mm) of IPM	MIC (µg/mL) of IPM	Category	Biofilm (OD 590 nm)
Kp1	25 ± 3.2	0.24	S	0.28 ± 0.19
Kp2	14 ± 1.9	62.5	R	0.60 ± 0.18
Kp3	21.1 ± 2.9	1.95	I	0.46 ± 0.14
Kp4	9.4 ± 1.5	250	R	0.77 ± 0.17
Kp5	24.5 ± 3.4	0.48	S	0.55 ± 0.13
Kp6	28.3 ± 4.8	0.24	S	0.47 ± 0.11
Kp7	16.8 ± 2.2	62.5	R	0.59 ± 0.26
Kp8	31.7 ± 3.2	0.24	S	0.23 ± 0.19
Kp9	9.3 ± 0.8	250	R	0.79 ± 0.28
Kp10	12 ± 1.6	125	R	0.68 ± 0.22
Kp11	24 ± 3.6	0.97	S	0.27 ± 0.21
Kp12	17 ± 3.2	31.25	R	0.43 ± 0.16
Kp13	12 ± 1.2	62.5	R	0.59 ± 0.26
Kp14	7.5 ± 0.8	250	R	0.82 ± 0.30
Kp15	15 ± 1.7	15.6	R	0.53 ± 0.15
Kp16	27 ± 3.6	0.48	S	0.40 ± 0.13
Kp17	25 ± 3.8	0.97	S	0.64 ± 0.15
Kp18	18 ± 2.6	15.6	R	0.60 ± 0.11
Kp19	11 ± 1.3	125	R	0.62 ± 0.24
Kp20	8.1 ± 1.4	250	R	0.73 ± 0.21

Biofilm formation and IPM response

Table 1 shows that all studied isolates produced biofilm to varying extents, with optical density values ranging from 0.23 ± 0.19 to 0.82 ± 0.30. Based on biofilm production, 14 (70%) of the *K. pneumoniae* isolates were classified as strong biofilm producers, 5 (25%) as moderate producers, and 1 (5%) as a weak biofilm producer. The study showed that susceptible isolates had low to moderate biofilm production ($OD_{590} \approx 0.27–0.47$), the intermediate isolate (Kp3) had moderate biofilm formation ($OD_{590} = 0.46 \pm 0.13$), while resistant isolates had moderate to strong biofilm formation ($OD_{590} \approx 0.53–0.82$). The relatively high SD observed for Kp1 (0.28 ± 0.19) reflects biological variability in biofilm production between experimental replicates, which is characteristic of weak biofilm producers exhibiting inconsistent surface attachment behavior.

Figure 1 shows a strong correlation between biofilm formation and IPM inhibition zone diameters (r = –0.819, p = 0.00096; Fig. 1A), highlighting increased resistance in high-biofilm-producing isolates. However, a significant positive correlation was observed between biofilm formation and IPM MICs in 20 isolates of *K. pneumoniae* (r = 0.79, p = 0.00024; Fig. 1B). The current findings show a significant association between increased biofilm formation and increased IPM resistance in *K. pneumoniae*.

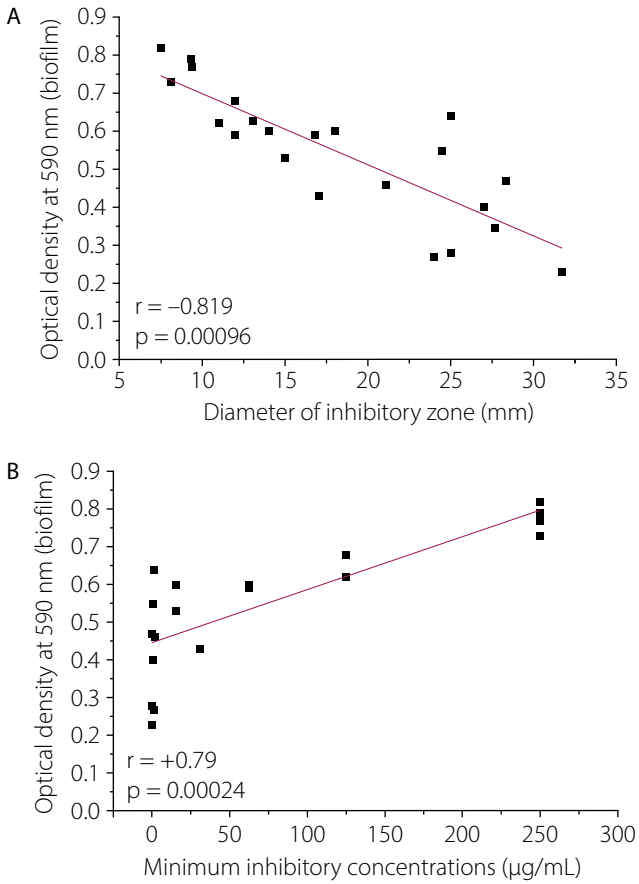

Fig. 1. Correlation between biofilm formation, expressed as crystal violet absorbance at 590 nm, and inhibition zone diameters of IPM against 20 *K. pneumoniae* isolates (A), as well as MIC values (B).

r – Pearson correlation coefficient; $p < 0.05$.

ZnO NPs preparation and characterization

Figure 2A shows an atomic force microscopy (AFM) image of the surface topography of the synthesized ZnO NPs. The nanoparticles are uniformly distributed and have diameters of less than 50 nm, indicating successful preparation. The three-dimensional distribution shows that most particles are spherical to slightly irregular aggregated structures. Figure 2B shows a scanning electron microscopy (SEM) image of ZnO nanoparticles at × 100,000 magnification (scale bar = 500 nm). The nanoparticles exhibited an almost spherical morphology with slight agglomeration. The particle size observed in SEM is consistent with AFM measurements, confirming nanoscale dimensions below 50 nm. Overall, both AFM and SEM analyses confirm the successful synthesis of ZnO nanoparticles with nanoscale size, uniform dispersion, and typical spherical morphology, suitable for further physicochemical and biological applications.

MTT assay

The cytotoxic effect of ZnO nanoparticles on MCF-7 breast cancer cells, assessed by the MTT assay, was demonstrated in this study. Figure 3A shows that MCF-7 cells were exposed to increasing concentrations of ZnO NPs (0–100 µg/mL) for 24 h, and cell viability was measured by determining the optical density (OD) at 570 nm. A concentration-dependent reduction in metabolic activity was observed. The greatest decrease in cancer cell viability was observed at higher ZnO NP concentrations (25, 50, and 100 µg/mL) compared with the untreated control (0 µg/mL). Data are presented as mean ± SD, and statistically significant differences relative to the control are indicated by asterisks (*, $p < 0.05$). Figure 3B shows the concentration–response curve, presenting percentage cell viability as a function of the $\log_{10}$ concentration of ZnO NPs. The half-maximal inhibitory concentration (IC_{50}) was determined to be 47.9 µg/mL, confirming the moderate cytotoxic effect of ZnO NPs against MCF-7 cells.

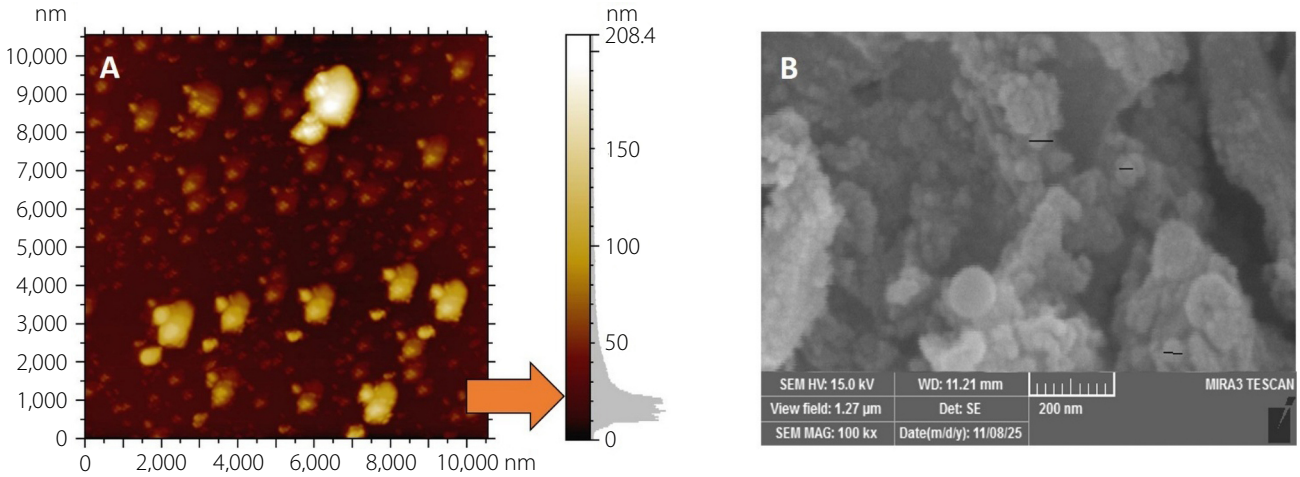

Fig. 2. A. Atomic force microscopy (AFM) 2D topography image of the ZnO nanoparticle (ZnO NP) surface. The orange arrow indicates the particle diameter, which is below 50 nm; B. Scanning electron microscopy (SEM) image of ZnO NPs at ×100,000 magnification (scale bar = 500 nm). The black bars confirm particle sizes below 50 nm

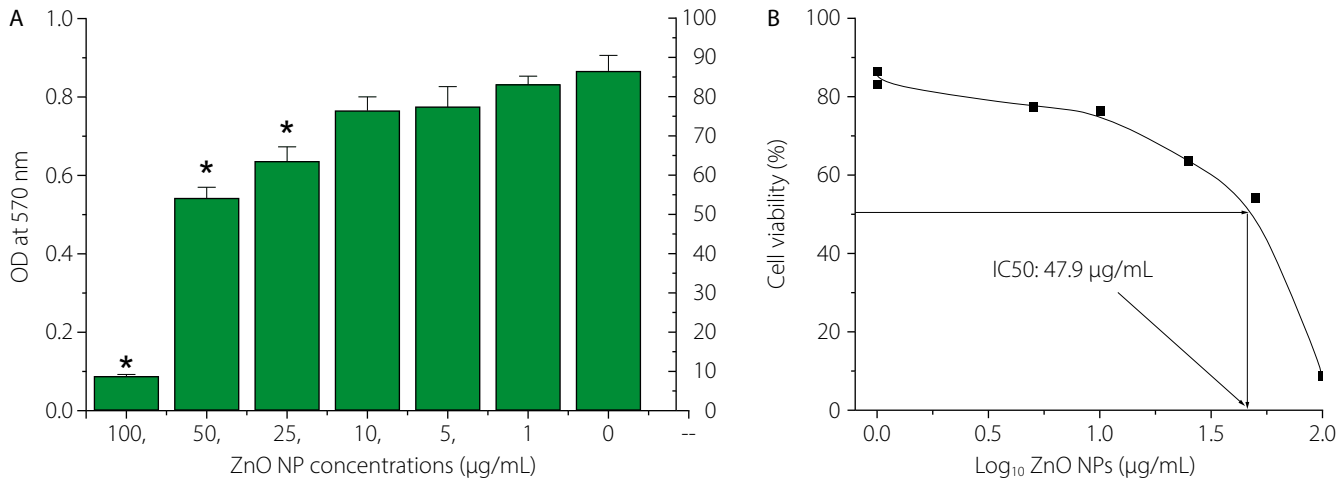

Fig. 3. Cytotoxic effect of ZnO NPs on MCF-7 cells assessed by the MTT assay. A. MCF-7 breast cancer cells were treated with increasing concentrations of ZnO NPs (0–100 µg/mL) for 24 h, and cell viability was evaluated by measuring optical density (OD) at 570 nm. Data are presented as mean ± SD. Asterisks indicate significant differences compared with the untreated control ($p < 0.05$); B. Concentration–response curve showing percentage cell viability plotted against the $\log_{10}$ concentration of ZnO nanoparticles. The half-maximal inhibitory concentration (IC_{50}) was 47.9 µg/mL

Effect of sub-MICs of IPM on biofilm formation

Figure 4 shows the impact of sub-MICs of IPM on biofilm formation in imipenem-resistant *K. pneumoniae* (IRKP) isolates (12 isolates), which strongly produced biofilm biomass. Across the isolates, biofilm biomass increased as the imipenem concentration decreased from ½ MIC to ⅟₃₂ MIC. The strongest biofilm production was observed when the isolates were exposed to the lowest antibiotic concentrations (⅟₁₆ and ⅟₃₂ MIC), with several isolates approaching control levels. However, higher antibiotic concentrations (½ and ¼ MIC) resulted in lower biofilm biomass formation. The highest concentrations of IPM (½, ¼, and ⅛ MICs) significantly reduced biofilm formation compared with the control in *K. pneumoniae* isolates not exposed to IPM ($p < 0.05$).

Effect of sub-MICs of ZnO NPs on biofilm formation

Figure 5 shows the concentration-dependent inhibitory effect of ZnO NPs on biofilm biomass formation by 12 isolates of *K. pneumoniae* on polystyrene microtiter plates. Exposure to ZnO NPs decreased biofilm biomass. The highest concentration (½ MIC) produced the most significant inhibition compared with the control ($p < 0.05$). The antibiofilm effect of ZnO NPs decreased with decreasing concentrations of ZnO NPs (¼ MIC to ⅟₃₂ MIC). Strong biofilm producers showed a decrease in biofilm production even at lower ZnO NP concentrations up to ⅟₁₆ MIC ($p < 0.05$). These data demonstrate that ZnO NPs exhibit significant concentration-dependent antibiofilm activity against *K. pneumoniae*.

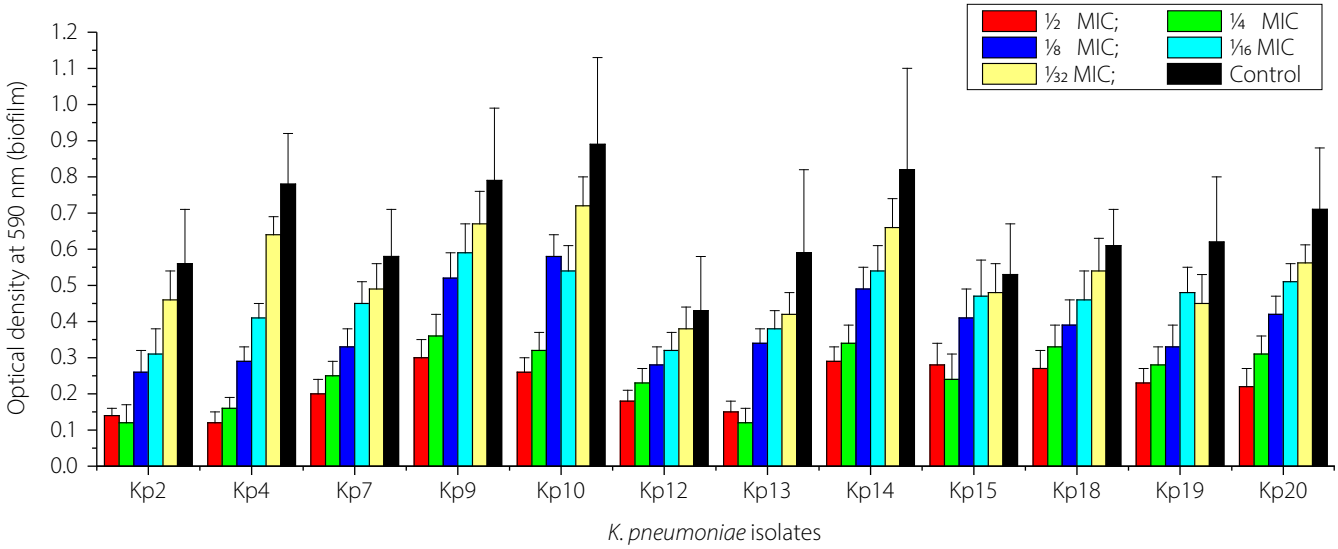

Fig. 4. Effect of sub-minimum inhibitory concentrations (sub-MICs) of imipenem (IPM) on biofilm formation by 12 *K. pneumoniae* isolates on polystyrene microtiter plates. The antibiofilm effect of sub-MICs of IPM was concentration dependent. Y-axis, biofilm biomass (OD_{590}); X-axis, *K. pneumoniae* isolates. Data are presented as mean ± SD

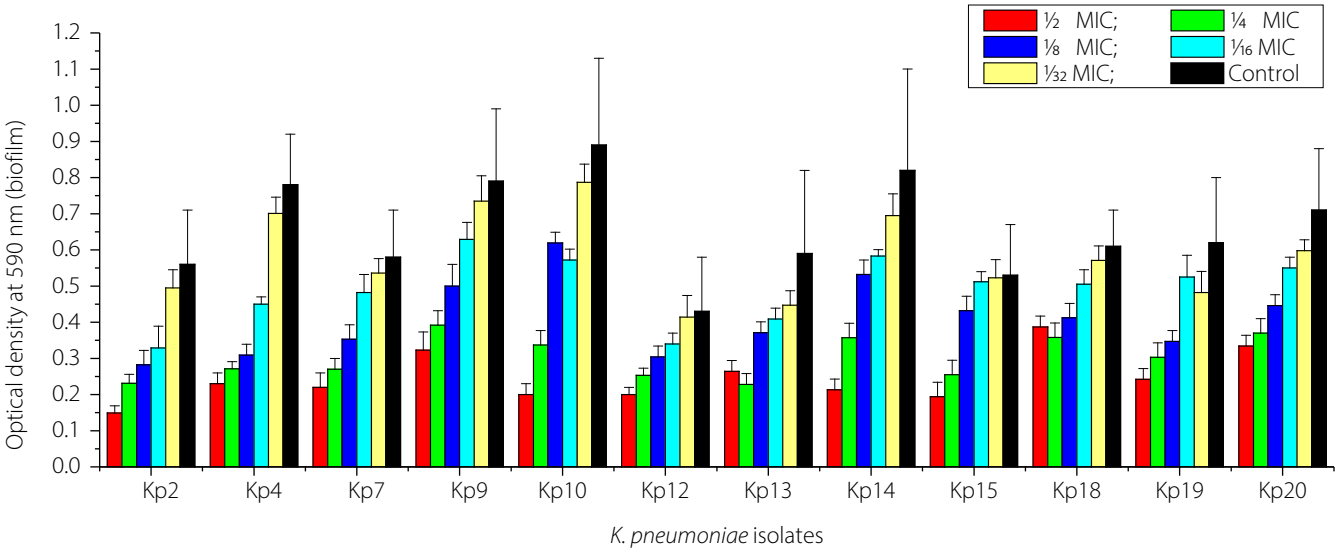

Fig. 5. Concentration-dependent inhibition of *K. pneumoniae* biofilm formation by zinc oxide nanoparticles (ZnO NPs). Biofilm formation by 12 *K. pneumoniae* isolates on polystyrene was quantified as optical density at 590 nm. Isolates were treated with sub-MICs of ZnO NPs (½, ¼, ⅛, ⅟₁₆, and ⅟₃₂ MIC). Y-axis, biofilm biomass (OD_{590}); X-axis, *K. pneumoniae* isolates. Data are presented as mean ± SD

Additive effect of ZnO NPs and IPM on MICs

The effect of different concentrations of ZnO NPs (sub-MICs) on the susceptibility of Kp14 (*K. pneumoniae* isolate exhibiting the highest level of biofilm formation and resistance to IPM) to IPM is shown in Fig. 6. The results showed that all tested sub-MICs of ZnO NPs significantly reduced ($p < 0.05$) the minimum inhibitory concentration (MIC) of IPM required to completely inhibit the growth of Kp14, compared with the control treatment (MICs of IPM without ZnO NPs). The greatest decreases in the MIC of IPM were observed in the presence of ½ MIC, ¼ MIC, and ⅛ MIC of ZnO NPs. These concentrations of ZnO NPs reduced the MIC of IPM against Kp14 from 250 ± 50 µg/mL to 116.6 ± 14.4 µg/mL, while 1/16 MIC of ZnO NPs decreased the MIC of IPM from 250 ± 50 µg/mL to 125 ± 25 µg/mL. Furthermore, 1/32 and 1/64 MICs of ZnO NPs reduced the MIC of IPM against Kp14 from 250 ± 50 µg/mL to 141.6 ± 14.4 µg/mL and 158.3 ± 80.36 µg/mL, respectively. Despite the reduction in MIC values, Kp14 remained classified as clinically resistant to IPM, as the post-treatment MICs substantially exceeded the CLSI susceptibility breakpoint of ≤1 µg/mL. These findings are therefore described as ZnO NPs potentiating imipenem activity, rather than fully restoring susceptibility.

The fractional inhibitory concentration index (FICI) was calculated for each ZnO NP sub-MIC concentration tested (Table 2). FICI values ranged from approximately 0.97 (at ½ MIC ZnO NPs) to 1.13 (at 1/64 MIC ZnO NPs), indicating additive interactions across all tested concentrations. A FICI ≤ 0.5 is defined as synergistic, 0.5–1.0 as additive, 1.0–2.0 as indifferent, and > 2.0 as antagonistic. The results therefore confirm an additive potentiation effect rather than classical synergy.

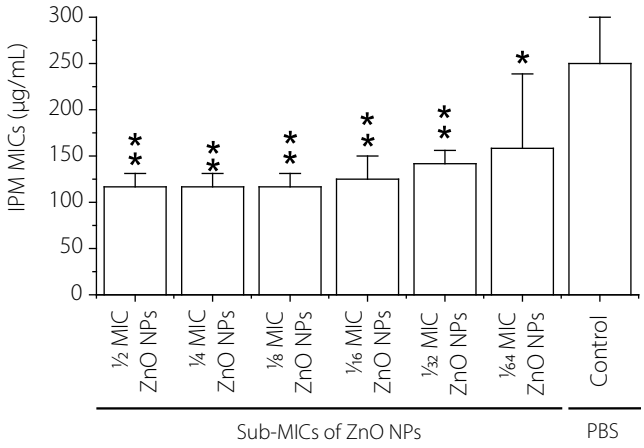

Fig. 6. Additive effect of sub-inhibitory concentrations (½ MIC, ¼ MIC, ⅛ MIC, 1/16 MIC, 1/32 MIC, and 1/64 MIC) of ZnO NPs on reducing the MIC of IPM against Kp14. Asterisks indicate significant differences compared with the control (MIC of IPM against Kp14 with Sub-MICs of ZnO NPs): *$p < 0.05$; **$p < 0.005$.

Additive effect of ZnO NPs and imipenem on biofilm formation

Table 3 shows the effect of sub-inhibitory concentrations of ZnO NPs and IPM on biofilm formation by Kp14. The results showed the highest inhibition of biofilm formation when Kp14 was exposed to ½ MIC of ZnO NPs and ½ MIC of IPM compared with three controls (first, second, and third controls). The lowest inhibition of biofilm formation was observed when the bacterial isolate (Kp14) was

Table 2. Fractional inhibitory concentration index (FICI) values for the combination of ZnO NPs and IPM against Kp14, calculated using the checkerboard microdilution assay. FICI = (MIC of IPM in combination/MIC of IPM alone) + (concentration of ZnO NPs used/MIC of ZnO NPs alone). Interpretation: ≤0.5, synergistic; 0.5–1.0, additive; 1.0–2.0, indifferent; >2.0, antagonistic

¼ MIC ZnO NPs	116.6 ± 14.4	0.72	Additive
1/16 MIC ZnO NPs	125 ± 25	0.81	Additive
1/64 MIC ZnO NPs	158.3 ± 80.4	1.13	Indifferent

Table 3. Biofilm formation, expressed as optical density at 590 nm, of *K. pneumoniae* (Kp14) after incubation for 24 h at 37°C under exposure to sub-MICs of ZnO NPs, sub-MICs of imipenem (IPM), and their combination. First control, biofilm formation of Kp14 under exposure to sub-MICs of IPM; second control, biofilm formation of Kp14 under exposure to sub-MICs of ZnO NPs; third control, biofilm formation of Kp14 without exposure to sub-MICs of IPM or ZnO NPs. #$p < 0.05$ vs first control; ^$p < 0.05$ vs second control; *$p < 0.05$ vs third control

Sub-MICs of ZnO NPs	½ MIC of IPM	¼ MIC of IPM	⅛ MIC of IPM	1/16 MIC of IPM	1/32 MIC of IPM	1/64 MIC of IPM	2nd control
½ MIC of ZnO NPs	0.14 ± 0.05*#^	0.18 ± 0.04*#^	0.19 ± 0.03*#^	0.20 ± 0.04*#^	0.22 ± 0.05*#^	0.23 ± 0.06*#^	0.33 ± 0.03
¼ MIC of ZnO NPs	0.16 ± 0.04*#^	0.19 ± 0.05*#^	0.20 ± 0.04*#^	0.23 ± 0.05*#^	0.26 ± 0.06*#^	0.31 ± 0.07*#	0.357 ± 0.04
⅛ MIC of ZnO NPs	0.19 ± 0.05*#^	0.17 ± 0.04*#^	0.21 ± 0.05*#^	0.24 ± 0.05*#^	0.31 ± 0.06*#^	0.39 ± 0.08*#^	0.532 ± 0.04
1/16 MIC of ZnO NPs	0.17 ± 0.05*#^	0.21 ± 0.05*#^	0.20 ± 0.06*#^	0.25 ± 0.06*#^	0.35 ± 0.07*#^	0.48 ± 0.09*#^	0.583 ± 0.0177
1/32 MIC of ZnO NPs	0.19 ± 0.05*#^	0.20 ± 0.05*#^	0.21 ± 0.04*#^	0.26 ± 0.06*#^	0.32 ± 0.08*#^	0.51 ± 0.10*#^	0.695 ± 0.06
1/64 MIC of ZnO NPs	0.15 ± 0.04*#^	0.20 ± 0.06*#^	0.23 ± 0.05*#^	0.29 ± 0.06*#^	0.39 ± 0.09*#	0.59 ± 0.11*#^	0.701 ± 0.04
1st control	0.29 ± 0.04	0.34 ± 0.05	0.49 ± 0.06	0.54 ± 0.07	0.66 ± 0.08	0.70 ± 0.102	0.83 ± 0.23 (3rd control)

exposed to ¼ sub-MICs of both agents (ZnO NPs and IPM), although these concentrations still reduced biofilm formation significantly compared with the three controls. The present study, for the first time, shows that sub-MICs of IPM and ZnO NPs in combination reduce biofilm formation by Kp14 (IRKP) more than exposure to either sub-MIC alone. The present study confirms the synergistic effect of sub-inhibitory concentrations of ZnO NPs in reducing biofilm formation by Kp14 under sub-MIC IPM stress. This finding explains one mechanism by which ZnO NPs reduce Kp14 resistance to IPM.

Discussion

The growing resistance of pathogenic bacteria to a wide range of antibiotics has become a significant global challenge and represents a serious public health threat. Moreover, no new effective antibiotics have been discovered in recent years to counteract the increasing proportion of antibiotic-resistant bacteria. The recent World Health Organization report has classified carbapenem (imipenem)-resistant bacteria as a high priority for the development of new antimicrobials. Carbapenem-resistant *K. pneumoniae* (CRKP) infections are associated with mortality rates exceeding 28.7% in hospitalized patients, particularly among immunocompromised individuals with pneumonia and sepsis.[22] The emergence and spread of infections caused by multidrug-resistant (MDR) or extensively drug-resistant (XDR) bacteria increase the risk of morbidity and mortality among infected patients.[23,24]

The present study elucidates the moderate incidence of *K. pneumoniae* in urinary tract infections (UTIs). The incidence of UTIs caused by *K. pneumoniae* is 16.2% in Iraq, and it is the second most common uropathogen, accounting for 15% to 23% of culture-positive UTIs.[25] Sub-inhibitory concentrations of imipenem and ZnO NPs, applied separately, reduced biofilm formation by imipenem-resistant *K. pneumoniae* (IRKP) on polystyrene microtiter plates. The novelty of the current study lies in demonstrating the enhancing effect of ZnO NPs on the antibacterial activity of imipenem (IPM) against IRKP, as well as their combined antibiofilm effect. However, despite this enhancement, the increased bacterial susceptibility did not reach the threshold for clinical susceptibility to imipenem, as MIC values decreased from 250 ± 50 μg/mL to 116.6 ± 14.4 μg/mL, still exceeding the CLSI susceptibility breakpoint of ≤1 μg/mL.[13] These findings offer a promising strategy to combat the growing challenge of antimicrobial resistance in this opportunistic pathogen.

The strong negative correlation between biofilm formation and inhibition zone diameter (r = −0.819) directly supports the established barrier function of the extracellular polymeric substance (EPS) matrix. The EPS matrix physically restricts antibiotic diffusion, reduces the local antibiotic concentration at the bacterial cell surface, and creates a microenvironment characterized by reduced pH and oxygen tension, which further diminishes antibiotic efficacy. Collectively, these factors explain the observed inverse relationship between biofilm production and IPM susceptibility.

It is important to note that although ZnO NPs significantly reduced the MIC of IPM against Kp14, the post-treatment MIC still substantially exceeds the CLSI susceptibility breakpoint of ≤1 μg/mL for IPM. Therefore, these findings are more accurately described as ZnO NPs potentiating imipenem activity rather than fully restoring susceptibility. This potentiation effect, while not sufficient to reclassify the isolate as clinically susceptible, may contribute to improved clinical outcomes when higher antibiotic concentrations are achieved at the site of infection. Clinically, this implies that the concentrations required to achieve meaningful IPM potentiation would substantially exceed standard therapeutic doses, and thus the current findings cannot be directly translated into revised dosing recommendations without extensive pharmacokinetic/pharmacodynamic (PK/PD) modeling and in vivo validation. Nevertheless, the demonstrated potentiation provides proof of concept that ZnO NPs can modulate carbapenem activity through membrane permeabilization and biofilm disruption.

The cytotoxicity of ZnO NPs against MCF-7 cells yielded an IC_{50} of 47.9 μg/mL. Importantly, the sub-MIC concentrations of ZnO NPs used in the synergy experiments were substantially below this IC_{50} value, suggesting a potential therapeutic safety margin. This differential selectivity – antibacterial activity at concentrations below the eukaryotic cytotoxic threshold – is an essential consideration in evaluating ZnO NPs as candidate adjunct antimicrobial agents. However, in vivo validation of this safety margin remains necessary prior to clinical translation.

Thymus vulgaris was selected as the green synthesis agent for ZnO NPs based on its well-documented phytochemical profile, particularly its high content of thymol, carvacrol, and flavonoids, which function as reducing and capping agents during nanoparticle biosynthesis. These phenolic compounds stabilize the nanoparticle surface, control particle size, and may also contribute residual antimicrobial activity. Furthermore, *Thymus vulgaris* extracts are widely available, low-cost, non-toxic, and environmentally sustainable compared with chemical reducing agents, aligning with the green chemistry principles that guided this study.

The synergistic antibacterial activity can be explained by multiple mechanisms of action of ZnO NPs. Previous studies have reported that ZnO NPs can induce oxidative stress by generating reactive oxygen species (ROS), such as superoxide and hydroxyl radicals.[26,27] These reactive species lead to lipid peroxidation, protein denaturation, and DNA damage, ultimately disrupting cellular structure and bacterial function.[28] Furthermore, the dissolution of ZnO NPs releases Zn^{2+} ions that interfere with key cellular enzymatic processes, disrupt membrane potential, and suppress

essential bacterial cell functions.[29] The interaction of ZnO NPs with protein components of the bacterial cell membrane enhances membrane damage, increases membrane permeability, and facilitates the uptake of antibiotics.[30] This increased permeability likely plays a significant role in the observed potentiation, enabling IPM to reach its intracellular targets more effectively.

In addition to planktonic growth, the combined effect of ZnO NPs and IPM inhibits *K. pneumoniae* biofilm formation in vitro. The primary role of biofilms is to promote bacterial resistance to antibiotics and host immune responses by reducing antibiotic penetration and decreasing the effectiveness of phagocytic cells in clearing bacterial cells in vivo.[31] Several previous studies have shown that ZnO NPs exhibit antibiofilm activity by disrupting the extracellular polymeric substance (EPS) matrix, reducing bacterial adhesion to surfaces, and interfering with quorum-sensing mechanisms.[32,33] The combination of ZnO NPs and imipenem enhances these effects, as compromised bacterial cells within the biofilm matrix become more susceptible to both agents, leading to disruption of the biofilm structure. This is consistent with previous findings showing that other carbapenems (e.g., meropenem) exhibit antibiofilm activity when combined with ZnO NPs against carbapenem-resistant *K. pneumoniae*.[34]

These outcomes have important implications. *K. pneumoniae* is one of the pathogens responsible for hospital-acquired infections, and carbapenem-resistant isolates, particularly IRKP, represent a serious threat to public health.[23,24,35,36] The combined effect of ZnO NPs and IPM reduces the effective imipenem dose required for treatment, potentially decreasing antibiotic-associated toxicities and slowing the progression of further resistance. This line of research is therefore highly relevant for addressing multidrug resistance. The current study highlights the need for further research to clarify the mechanisms underlying the enhancing effect of ZnO NPs on imipenem activity. Molecular studies should investigate the roles of genes associated with *K. pneumoniae* resistance to imipenem, as well as those involved in biofilm formation and polymerization. Such studies may help elucidate how the combined action of these agents improves antibiotic efficacy. Another important aspect is the need for in vivo validation of the enhancing effect of ZnO NPs on imipenem activity in infections caused by carbapenem-resistant bacteria, which remain a major public health concern. Future in vivo studies will employ a murine UTI model (transurethral instillation of *K. pneumoniae* in C57BL/6 mice) to evaluate the efficacy and safety of combined ZnO NP and imipenem treatment, consistent with established models for carbapenem-resistant *K. pneumoniae* infections. These limitations are being addressed in ongoing research projects in our laboratory.

Conclusions

The present study determined the incidence of UTIs caused by *K. pneumoniae* resistant to IPM. A significant relationship was observed between the ability of *K. pneumoniae* to form biofilms and its resistance to IPM. Sub-MICs of IPM and ZnO NPs significantly reduced biofilm formation. The current study demonstrates, for the first time, the additive effect of sub-MIC ZnO NPs in reducing biofilm formation and potentiating imipenem activity against *K. pneumoniae*. These findings suggest the potential use of ZnO NPs to enhance the effectiveness of IPM against IPM-resistant *K. pneumoniae*.

ORCID iDs

Deyar Jassim Shawi 0009-0005-2234-6592
Ayaid Khadem Zgair 0000-0002-2356-3338

References

1. Nagham SM, Obaid MM, Jasem MJ, Noaman TM. Impact of biofilm formation on antibiotic resistance in *Escherichia coli*. *World J Exp Biosci*. 2024;12(2):44–48. doi:10.65329/wjeb.v12.02.004
2. Campos JV, Pontes JTC, Canales CSC, Roque-Borda CA, Pavan FR. Advancing nanotechnology: Targeting biofilm-forming bacteria with antimicrobial peptides. *BME Front*. 2025;6:0104. doi:10.34133/bmef.0104
3. Hajareh Haghighi F, Mercurio M, Cerra S, et al. Surface modification of TiO_2 nanoparticles with organic molecules and their biological applications. *J Mater Chem B*. 2023;11(11):2334–2366. doi:10.1039/D2TB02576K
4. Hosnedlova B, Kabanov D, Kepinska M, et al. Effect of biosynthesized silver nanoparticles on bacterial biofilm changes in *S. aureus* and *E. coli*. *Nanomaterials*. 2022;12(13):2183. doi:10.3390/nano12132183
5. Fu Y, Zhang Y, Zhao J, et al. Emergence of co-resistance to imipenem/relebactam and ceftazidime/avibactam in clinical *Klebsiella pneumoniae* ST11 clone due to KPC-2 N132S and CTX-M-65 S130G/P167S substitutions. *Antimicrob Agents Chemother*. 2025;69(12):e00891-25. doi:10.1128/aac.00891-25
6. Chen HQ, Mo ZH, Wei WX. Case report: Trauma-induced *Klebsiella pneumoniae* invasive syndrome presenting with liver abscess, lung abscess, endophthalmitis, and purulent meningitis. *Front Med (Lausanne)*. 2025;11:1513831. doi:10.3389/fmed.2024.1513831
7. Mendes G, Santos ML, Ramalho JF, Duarte A, Caneiras C. Virulence factors in carbapenem-resistant hypervirulent *Klebsiella pneumoniae*. *Front Microbiol*. 2023;14:1325077. doi:10.3389/fmicb.2023.1325077
8. Ashaduzzaman M, Al Muhit MA, Dey SC, et al. Microwave assisted starch stabilized green synthesis of zinc oxide nanoparticles for antibacterial and photocatalytic applications. *Sci Rep*. 2025;15(1):28288. doi:10.1038/s41598-025-14193-8
9. Masadeh MM, Bany-Ali NM, Khanfar MS, Alzoubi KH, Masadeh MM, Al Momany EM. Synergistic antibacterial effect of ZnO nanoparticles and antibiotics against multidrug-resistant biofilm bacteria. *Curr Drug Deliv*. 2025;22(1):92–106. doi:10.2174/0115672018279213240110045557
10. Rodríguez-Suárez JM, Gershenson A, Onuh TU, Butler CS. The heterogeneous diffusion of polystyrene nanoparticles and the effect on the expression of quorum-sensing genes and EPS production as a function of particle charge and biofilm age. *Environ Sci Nano*. 2023;10(9):2551–2565. doi:10.1039/D3EN00219E
11. Norouzalinia F, Asadpour L, Mokhtary M. Anti-microbial, anti-biofilm, and efflux pump inhibitory effects of ellagic acid–bonded magnetic nanoparticles against *Escherichia coli* isolates. *Int Microbiol*. 2024;28(3):563–573. doi:10.1007/s10123-024-00560-4
12. Talib MM, Ghafil JA. Comparative adhesion of *Pseudomonas aeruginosa* to human oral mucosal epithelial cells and polystyrene surfaces. *J Fac Med Baghdad*. 2024;66(3):344–349. doi:10.32007/jfacmedbaghdad.6632328
13. Clinical and Laboratory Standards Institute (CLSI). *CLSI M100. Performance Standards for Antimicrobial Susceptibility Testing*. 34th ed. Malvern, USA: Clinical and Laboratory Standards Institute (CLSI); 2024. ISBN: 978-1-68440-305-9, 978-1-68440-306-6.

14. Karam ST, Abdulrahman AF. Green synthesis and characterization of ZnO nanoparticles by using thyme plant leaf extract. *Photonics*. 2022;9(8):594. doi:10.3390/photonics9080594
15. Sadiq SI, Ghafil JA. Polyhydroxybutyrate nanoparticle improving the sensitivity of *Pseudomonas aeruginosa* to ceftriaxone and reducing the biofilm formation in vitro. *Polim Med*. 2025;55(1):31–39. doi:10.17219/pim/203765
16. Mosmann T. Rapid colorimetric assay for cellular growth and survival: Application to proliferation and cytotoxicity assays. *J Immunol Methods*. 1983;65(1–2):55–63. doi:10.1016/0022-1759(83)90303-4
17. Plumb JA. Cell sensitivity assays: The MTT assay. *Methods Mol Med*. 1999;28:25–30. doi:10.1385/1-59259-687-8:25
18. Berridge MV, Herst PM, Tan AS. Tetrazolium dyes as tools in cell biology: New insights into their cellular reduction. *Biotechnol Annu Rev*. 2005;11:127–152. doi:10.1016/S1387-2656(05)11004-7
19. Abd Al-Mutalib L, Zgair A. Effect of subinhibitory doses of rifaximin on in vitro *Pseudomonas aeruginosa* adherence and biofilm formation to biotic and abiotic surface models. *Polim Med*. 2023;53(2):97–103. doi:10.17219/pim/166584
20. Talib MM, Ghafil JA. Effect of sub-minimum inhibitory concentrations of ceftriaxone on the *Pseudomonas aeruginosa* adhesion to human oral mucosal epithelial cells and biofilm formation to polystyrene in vitro. *Pharm Sci Asia*. 2024;51(2):180–189. doi:10.29090/psa.2024.02.24.1752
21. Mohammed HA, Zgair AK. Detection of quorum sensing genes of *Pseudomonas aeruginosa* isolated from different areas in Iraq. *Iraqi J Sci*. 2022;63(11):4665–4673. doi:10.24996/ijs.2022.63.11.5
22. Zhou C, Sun L, Li H, Huang L, Liu X. Risk factors and mortality of elderly patients with hospital-acquired pneumonia of carbapenem-resistant *Klebsiella pneumoniae* infection. *Infect Drug Resist*. 2023;16:6767–6779. doi:10.2147/IDR.S431085
23. World Health Organization (WHO). *WHO Bacterial Priority Pathogens List 2024: Bacterial Pathogens of Public Health Importance, to Guide Research, Development, and Strategies to Prevent and Control Antimicrobial Resistance*. Geneva, Switzerland: World Health Organization (WHO); 2024. ISBN:978-92-4-009346-1.
24. Mondol SM, Islam MdR, Mia MdE, et al. Molecular and genomic insights into multidrug-resistant (MDR) and extensively drug-resistant (XDR) *Pseudomonas aeruginosa* causing burn wound infections in Bangladesh. *Sci Rep*. 2025;15(1):32629. doi:10.1038/s41598-025-19576-5
25. Polse RF, Qarani SM, Assafi MS, Sabaly N, Ali F. Incidence and Antibiotic Sensitivity of *Klebsiella pneumoniae* isolated from urinary tract infection patients in Zakho emergency hospital/Iraq. *J Educ Sci*. 2020;29(3):257–268. doi:10.33899/edusj.2020.126827.1056
26. Mendes CR, Dilarri G, Forsan CF, et al. Antibacterial action and target mechanisms of zinc oxide nanoparticles against bacterial pathogens. *Sci Rep*. 2022;12(1):2658. doi:10.1038/s41598-022-06657-y
27. Sirelkhatim A, Mahmud S, Seeni A, et al. Review on zinc oxide nanoparticles: Antibacterial activity and toxicity mechanism. *Nanomicro Lett*. 2015;7(3):219–242. doi:10.1007/s40820-015-0040-x
28. Jiang S, Lin K, Cai M. ZnO nanomaterials: Current advancements in antibacterial mechanisms and applications. *Front Chem*. 2020;8:580. doi:10.3389/fchem.2020.00580
29. Emram R, Sionov RV, Gutkin V, Wilensky A, Steinberg D, Assad R. Mechanism of action of zinc oxide nanoparticles as an antibacterial agent against *Streptococcus mutans*. *Biomolecules*. 2025;15(12):1660. doi:10.3390/biom15121660
30. Mahgoub SM, Mohamed EA, Aziz SAAA, et al. Synergistic potential of clindamycin hydrochloride loaded on zinc oxide nanoparticles: A novel approach to combat multidrug-resistant infections. *Sci Rep*. 2025;15(1):44665. doi:10.1038/s41598-025-30573-6
31. Mohamed AA, Saed S, El-Sayed SR, et al. A combined therapy of meropenem–ZnO nanoparticles efficiently eliminates carbapenem-resistant *Klebsiella pneumoniae* biofilms, with reduced nephrotoxicity (in vitro). *Lett Appl Microbiol*. 2024;77(12):ovae136. doi:10.1093/lambio/ovae136
32. Banerjee S, Vishakha K, Das S, et al. Antibacterial, anti-biofilm activity and mechanism of action of pancreatin doped zinc oxide nanoparticles against methicillin resistant *Staphylococcus aureus*. *Colloids Surf B Biointerfaces*. 2020;190:110921. doi:10.1016/j.colsurfb.2020.110921
33. Kumarage PM, Gul T, Green NJ, et al. Recent advances in gold and zinc oxide nanoparticles: Antibiofilm action, mechanisms beyond ROS generation, and in vivo efficacy. *Microbiol Res*. 2026;306:128441. doi:10.1016/j.micres.2026.128441
34. Mohsenzadeh A, Mohsenzadeh H, Mohammadi A, et al. Synergistic effects of zinc oxide nanoparticles and Meropenem on biofilm formation in *Pseudomonas aeruginosa*. *Cell Mol Biomed Rep*. 2025;5(2):121–134. doi:10.55705/cmbr.2025.481668.1280
35. Khan BK, Ud Din MA, Mohammed MT, Batool M, Ullah H. Antagonism and antibiofilm activity of sterile microbiota growth medium against *Klebsiella pneumoniae* in vitro. *World J Exp Biosci*. 2025;13(2):33–36. doi:10.65329/wjeb.v13.02.003
36. Ebrahimi FA, Siasi E, Yazdian F, Ashrafi F. Nanotechnology meets superbugs: Biocompatible polymeric nanoparticles combat MDR *Klebsiella pneumoniae* via gene suppression and biofilm inhibition. *Sci Rep*. 2025;15(1):37708. doi:10.1038/s41598-025-21606-1